Combined XPS and Contact Angle Studies of Flat and Rough Ethylene-Vinyl Acetate Copolymer Films

M. D. Doganci,[1] C. E. Cansoy,[1] I. O. Ucar,[1] H. Y. Erbil,[1] E. Mielczarski,[2] J. A. Mielczarski[2]

[1]*Gebze Institute of Technology, Department of Chemical Engineering, Cayirova, Gebze 41400, Kocaeli, Turkey*
[2]*LEM, Nancy-Université, CNRS, 15 avenue du Charmois B.P. 40 F-54501 Vandœuvre lès Nancy, France*

Received 26 January 2010; accepted 5 July 2011
DOI 10.1002/app.35189
Published online 26 October 2011 in Wiley Online Library (wileyonlinelibrary.com).

ABSTRACT: Flat and rough thin films were prepared by dip coating using LDPE, PVAc, and EVA polymers containing 12–40% VA contents. Surface free energy of flat films was determined by measuring contact angles. Surface atomic composition was investigated by XPS at 0° and 60° take-off angles. XPS results show that hydrophobic PE component was found to enrich at the near-surface region for all EVA samples for a depth of ~ 5 nm for both flat and rough surfaces, whereas hydrophilic VA component was enriched on the surface when VA < 18% for only at 10 nm depth. The difference between the XPS results of the flat and rough surfaces was not significant for EVA samples except EVA-33 surface where the atomic oxygen content decreased 15–20% for rough surfaces. Contact angle hysteresis values for the rough samples were much larger than that of the flat samples for LDPE and EVA-12 surfaces due to the presence of partial trapping of air pockets on these rough surfaces. A good agreement was obtained between surface concentration of atomic oxygen in the 5 nm outermost layer and γ_S^- surface free energy component especially for the samples having high VA contents. © 2011 Wiley Periodicals, Inc. J Appl Polym Sci 124: 2100–2109, 2012

Key words: ethylene-vinyl acetate copolymers; contact angle; XPS; surface free energy; polyolefin

INTRODUCTION

Thin coatings obtained from copolymers have different chemical compositions at the outermost surface layer when compared with their bulk structures. The surface composition of any coating is important in the adhesive, paint, and biomedical applications.[1–3] It is well known that the surface dynamics of polymers are considerably different from those of more rigid materials such as metals and ceramics, due to the high mobility of macromolecules at the surface. Hydrophobicity of a surface can be enhanced by chemical modifications, which lower the surface free energy, and also by physical modifications which increase the roughness of a surface. A superhydrophobic surface is defined as the surface having a water drop contact angle greater than 150°.[4] Superhydrophobic surfaces should have small contact angle hysteresis (the difference between advancing and receding contact angles, $\Delta\theta$) and low tilt angles where a water drop can roll spontaneously. Polypropylene (PP), which is a cheap polyolefin, was transformed into a superhydrophobic surface for the first time by using a simple solvent/nonsolvent phase separation method by Erbil et al. in 2003.[5] Later, Lu et al. applied the same phase separation method to obtain superhydrophobic surfaces from low-density polyethylene (LDPE).[6–8] Similarly, Kang et al. formed superhydrophobic LDPE surfaces having porous micro–nano binary morphology structures by using a simple casting method.[9] Yao et al. obtained micro/nm-scaled superhydrophobic surfaces with tunable sliding angles from isotactic PP.[10] Pakkanen and coworkers fabricated many superhydrophobic surfaces by using polyolefines.[11–13] They demonstrated that melt blending of HDPE with perfluoropolyethers permanently improves the hydrophobicity of the polyethylene. Modifications were done by injection molding and 2 wt % of liquid perfluoropolyethers was added to the melt HDPE and a nanoporous anodic aluminum oxide mold insert was used to obtain the nanopatterned surfaces with well-arranged, high aspect ratio nanostructure over the entire surface.[11] They also prepared polyethylene and polypropylene surfaces that were micro- or nanostructured or simultaneously micro- and nanostructured with the same method by adjusting the settings of a micro working robot and the parameters of the anodization procedure while preparing the aluminum oxide mold insert.[12,13] Recently, Ucar et al. prepared hydrophobic polyolefin surfaces by

Correspondence to: H. Y. Erbil (yerbil@gyte.edu.tr) or J. A. Mielczarski (jerzy.mielczarski@ensg.inpl-nancy.fr).

Contract grant sponsor: EC-6th Framework Integrated Project-AMBIO "Advanced Nanostructured Surfaces for the Control of Biofouling"; contract grant number: NMP4-CT-2005-011827.

using a dip coating method which were used in marine antifouling applications.[14]

Surface free energy of polymeric films can be determined by contact angle measurements of specific liquid drops on a flat solid surface, as was first proposed by Girifalco-Good[15] and Fowkes.[16] The presence of surface roughness makes this measurement more complicated and sometimes impossible. Owens and Wendt reported a simple method to calculate the surface free energy from contact angle measurements for flat surfaces by using only two liquids: water and methylene iodide.[17] Although, it is a useful method especially for nonpolar polymers, Owens-Wendt method gives erroneous results when hydrogen-bonding interactions are present between the polymer and the liquid drop. Later, van Oss, Good, and Chaudhury jointly developed a theory and a practical methodology to estimate the interfacial tension between nonpolar and electron-acceptor or electron-donor molecules in 1988.[18,19] They assumed that surface and interfacial free energies were consisted of two components; a nonpolar or a Lifshitz-van der Waals component (indicated by superscript LW) of electrodynamics origin and a polar component (indicated by superscript AB) caused by acid–base interactions. This methodology was successfully applied to calculate the magnitude of protein–liquid interactions and also the prediction of polymer solubility in solvents,[19] determining the surface free energy of polar and hydrogen bonding polymers. In addition, surface free energy versus bulk composition relationships of ester containing copolymers were successfully reported by using this method.[20]

On the other hand, when polymer surfaces are considerably rough, the application of Owens-Wendt and van Oss-Good-Chaudhury methods did not give reasonable results because of the trapped air pockets on the surface. Wenzel[21] and later Cassie and Baxter[22] showed that the introduction of roughness to a flat surface changes the contact angle results depending on the magnitude of the roughness and contact area fraction when air pockets are absent and complete wetting of the substrate takes place by the liquid drop. The increase of the roughness also increases the contact angle hysteresis ($\Delta\theta$) due to the pinning effect of the protrusions present on the surface when the drops are advancing. Chemical heterogeneity of the surface is another factor to increase the $\Delta\theta$ parameter and it is shown that copolymers having both nonpolar and polar pendant groups in the structure are chemically heterogeneous having large $\Delta\theta$ values.[1] Ethylene-vinyl acetate (EVA) random copolymer is a good example of this class. Nonpolar ethylene monomer ($CH_2{=}CH_2$) can be readily copolymerized with polar vinyl acetate monomer ($CH_2{=}CH{-}COO{-}CH_3$) to yield a range of ethylene-vinyl acetate (EVA) random copolymers having a wide variety of physical properties.[23] When the amount of VA in the copolymer is less than 40 wt %, the copolymer is referred to EVA, poly (ethylene-*co*-vinyl acetate), which is widely used as a hot melt adhesive and electrical insulator. When the amount of VA is more than 40 wt %, the copolymer is referred to VAE, poly (vinyl acetate-*co*-ethylene) which is widely used in film laminating and packaging adhesives in the form of emulsions.[3] EVA copolymers are less polar than polyvinyl acetate (PVAc) homopolymer, which is mainly produced by emulsion homo- and copolymerization to be used in adhesive and surface coating industries.[24] The incorporation of the polar VA comonomer units into a polyethylene backbone chain has many effects to change the final copolymer properties: Crystallinity, tensile yield strength, surface hardness, melting point of the polyethylene decreases and density, impact strength, optical clarity, glass transition temperature, gas permeability, coefficient of friction, and solubility in organic solvents increases with the increase in VA content.[23,25] Polar VA causes a corresponding change in compatibility with other suitable polymers and resins. The molecular weight and the ethylene sequence length decrease due to the increase of the VA content.[26] Semicrystalline EVA copolymers are used alone or blended with other plastics to form general molding and extrusion products where surface properties (such as adhesion, printability, wettability, and sealing) are critical to polymer performance.[25–31] The hydrophobicity of the copolymer surface varies depending on its bulk chemical composition, so that increasing the VA percentage in EVA copolymers decreases the equilibrium water contact angle, θ_e measured on polymer film surfaces and increases the total surface free energy, γ_{SV}^{Tot}. Matsunaga and Tamai[32] and later Erbil[33] determined the change of the surface free energy properties of EVA copolymer films with the copolymer composition from contact angle measurements. The surface free energy of polyethylene homopolymer was calculated by using the contact angles data by Dann et al.[34] and Park et al.[35] and it was determined that the results were in good agreement with the results obtained by applying the pendant drop shape method to PE melts.[36,37] Later, Grundke et al.[38] and Bistac et al.[39] also applied the van Oss-Good-Chaudhury method to determine the surface free energy of the EVA copolymers.

Although contact angles give a good idea on the hydrophobicity of a surface, they do not inform us the surface chemical composition. X-ray photoelectron spectroscopy (XPS) is one of the most important spectroscopic techniques to determine the chemical composition of a surface at nanometer scale. Briggs and Beamson reported the XPS studies of a wide

TABLE I
Characteristics of Polymers

Polymer	VA content (wt %)	MFI[a] (g/10 min) ASTM D1238 (2.16 kg, 190°C)	MFI (g/10 min) experimental (2.16 kg, 190°C)	Manufacturer	Commercial name
LDPE	0	4.1–5.4	4.85	PETKIM Petrochemicals	F5–21T
EVA-12	12	2.5	2.2	DuPont	ELVAX 660
EVA-18	18	1.8	1.8	Asia Polymer Corp.	EV101
EVA-28	28	5–8	5	Arkema	EVATANE
EVA-33	33	350–450	375	Arkema	EVATANE
EVA-40[b]	40	57	N/A	Aldrich	–
PVAc[b]	100	N/A	105	Aldrich	–

[a] Quoted from suppliers' catalogues.
[b] Molecular weights of EVA-40 and PVAc are 42,000[50] g/mol and 100,000 g/mol, respectively.

range of functional polymers containing carbonyl groups.[40] XPS can also be used to compare bulk and surface compositions of EVA copolymers that have varying oxygen atom percentages depending on VA content.[41–47] Chihani et al. analyzed EVA surfaces prepared by injection molding by using XPS.[41] The surface concentration of acetate groups was found to be higher than the bulk for EVA copolymers when perfluorinated ethylene propylene (FEP) was used as the mold.[41,43] Galuska characterized EVA+LDPE blend surfaces by using XPS and determined that VA content of the surface increases linearly with the bulk VA content.[42] McEvoy et al. investigated the fracture surfaces of interfaces between PE, PP, and EVA by XPS at three take-off angles and found that the fractured surfaces have greater percentage of VA than in the bulk at 1.5 nm penetrations.[27,44] XPS was used to determine the surface composition to investigate the adhesion properties of the surface-modified EVA copolymers[45] and also used to enhance the adhesion of EVA copolymers to polychloroprene with corona discharge.[46,47] In some instances, the XPS results correlate well with the surface free energy properties of polymer films determined from contact angles with the increase of polar comonomer ratio.[48]

The aim of this study is to investigate the effect of increasing the VA content in the bulk composition of the EVA copolymer to its final surface composition and wettability. In addition, the effect of surface roughness on the final surface composition is also considered. Thus, the surface chemical structure and wetting properties of both flat and rough EVA copolymer films are determined by using XPS and contact angle measurement and the results are discussed in the text.

EXPERIMENTAL

Materials

Low density polyethylene (LDPE) and polyvinyl acetate (PVAc) homopolymers and ethylene-vinyl acetate (EVA) copolymers were used for the preparation of flat and rough polymer surfaces. The names of manufacturers, VA contents (wt % in bulk) and melt flow index values (MFI) of the used polymers are given in Table I. All of the polymers were used as received. Standard glass slides (76 × 26 mm, ISOLAB, Turkey) were used in the dip-coating experiments.

Preparation of flat polymeric coatings

Glass slides were cleaned in chromic acid, rinsed with distilled water, and dried in an oven. All the homo- and copolymers were dissolved in technical xylene solvent (mixture of o-, m-, p- isomers, m- predominating) at specific temperatures to prepare the polymer solutions. The concentration of the LDPE solutions was 10 mg/mL and the concentration of all other copolymers and PVAc homopolymer was 40 mg/mL. Clean glass slides were dipped into the polymer solutions at varying temperatures from room temperature to 125°C by using a homemade mechanical dipper where the dipping speed can be precisely controlled. The sample preparation procedure by the dip coating technique is similar to as mentioned in the Ref. 14. The temperature during dipping was varied because of the solubility differences of the polymers in xylene solvent. Dipping temperatures and glass slide withdrawal rates are important parameters to obtain flat or rough polymer coating surfaces. Dipping temperature should be high and deposition rate should be low to achieve a flat coating. Glass slides were withdrawn from the polymer solutions at specific rates so that 612 mm/min rate was used for EVA-12 and EVA-40 solutions and 272 mm/min for all other EVA copolymers and PVAc, LDPE homopolymer solutions. Polymer-coated slides were dried in a vacuum oven overnight and kept in a desiccator before surface characterization. Film thicknesses for the flat coatings were determined from gravimetrical weight increase and were found to be within 0.3–1.0 μm.

TABLE II
Theoretical and Experimental Atomic Surface Concentrations of Carbon and Oxygen for Flat and Rough Polymer Samples Obtained by XPS at 0° and 60° Take-Off Angles

			Flat samples				Rough samples			
	Theoretical		0° take-off angle		60° take-off angle		0° take-off angle		60° take-off angle	
Polymer	*C*	*O*	*C*	*O*	*C*	*O*	*C*	*O*	*C*	*O*
LDPE	100	0	89.5	2.1	96.8	0.3	98.8	0.9	98.9	0.7
EVA-12	96.1	3.9	94.7	4.3	96.4	3.0	95.7	4.3	96.6	3.4
EVA-18	94.1	5.9	90.4	6.4	94.6	4.5	93.9	6.1	94.9	5.1
EVA-28	90.8	9.2	88.3	8.7	90.8	6.1	91.0	7.9	93.1	6.6
EVA-33	89.2	10.8	89.4	9.6	92.0	7.1	89.3	8.2	92.6	5.7
EVA-40	86.8	13.2	83.0	11.1	88.1	8.6	80.9	11.5	87.6	8.7
PVAc	66.7	33.3	71.0	26.9	75.4	21.1	N/A	N/A	N/A	N/A

Preparation of rough polymeric coatings

The procedure was similar to the flat coating preparation method; however, the concentrations were higher than that of the solutions giving flat coatings and varied between 40 and 100 mg/mL depending on the type of the copolymer to achieve a high surface roughness. Dipping temperatures should be low and deposition rates from the solution should be high to increase the roughness of the coating. Dipping temperatures varied between room temperature up to 100°C and the glass slide removal rates of 612 and 816 mm/min were applied during dip coating. (However, it is not possible to obtain a rough PVAc surface by dip-coating a glass slide into a PVAc homopolymer solution even at the room temperature). The film thicknesses for rough coatings were determined from gravimetrical weight increase and were found to be within 2.0–3.0 μm.

Surface characterization of polymer films

Contact angle measurements

Spectroscopic grades of water, methylene iodide, ethylene glycol, and formamide liquids which were purchased from MERCK were used in contact angle measurements. CAM 200 model of KSV Instruments, Finland contact angle meter was used to measure the static contact angles of the liquids under air. Equilibrium (θ_e) contact angles were measured by using 5 μL droplet volumes where the gravity flattening effect can be neglected. The needle was removed from the droplet during θ_e measurement and was kept within the liquid droplets during the advancing (θ_a) and receding (θ_r) contact angle measurements. A droplet of 3 μL volume was formed initially and its volume was increased up to 8 μL during the θ_a measurement. Then, the drop volume of 8 μL was decreased down to 3 μL while measuring θ_r. Measurements were made at three different locations for each polymer sample. Average contact angle and standard deviation values were found to be less than ±2.

Optical microscopy

Nikon SMZ 1500 Optical Microscope was used with X500 magnification to investigate the surface topography of all the coated samples.

X-ray photoelectron spectroscopy (XPS)

AXIS NOVA photoelectron spectrometer (Kratos Analytical, Manchester, UK) equipped with monochromatic AlKα ($hv = 1486.6$ eV) anode was used in the studies. The kinetic energy of the photoelectrons was determined with the hemispheric analyzer set to the pass energy of 160 eV for wide scan spectra and 20 eV for high-resolution spectra. Electrostatic charge effect of samples was overcompensated by means of the low-energy electron source working in combination with magnetic immersion lens. The carbon C1s line with position at 284.6 eV was used as a reference to correct the charging effect. Quantitative elemental compositions were determined from peak areas using experimentally determined sensitivity factors and spectrometer transmission function. Spectrum background was subtracted according to Shirley. The high-resolution spectra were analyzed by means of spectra deconvolution software (Vision 2, Kratos Analytical, UK).

In order to study the molecular structure of the top surface layers, i.e., a film of a few nanometers thickness, angle resolved XPS was applied and spectra were recorded for the two take-off angles of $\theta = 0°$ and 60°. The take-off angle is defined as the angle between the normal to the surface of the sample and the electron optical axis of the spectrometer. The effective information depth, varies according to $d = d_0 \cos \theta$, where d_o is the maximum information depth ($d_o \sim 10$ nm for the C1s line by employing an AlKα source). Uncertainty of the XPS measurements

was found to be less than 5% and we used one digit after comma in our reported XPS results which were presented in Table II.

RESULTS AND DISCUSSION

Optical microscopy

Indicative optical microscope images of some flat and rough copolymers at X500 magnification are given in Figure 1. When flat and rough surfaces are compared, the increase in the surface roughness was apparent for the rough samples, except EVA-40 copolymer as seen in Figure 1(b, d, and f). In addition, the presence of the spherulitic structures owing to the semicrystalline structure of LDPE was not seen with the increase of the VA content. rms roughness value which was determined from the AFM amplitude image by tapping mode was 16 nm for flat EVA-12 under air and is given in Ref. 14.

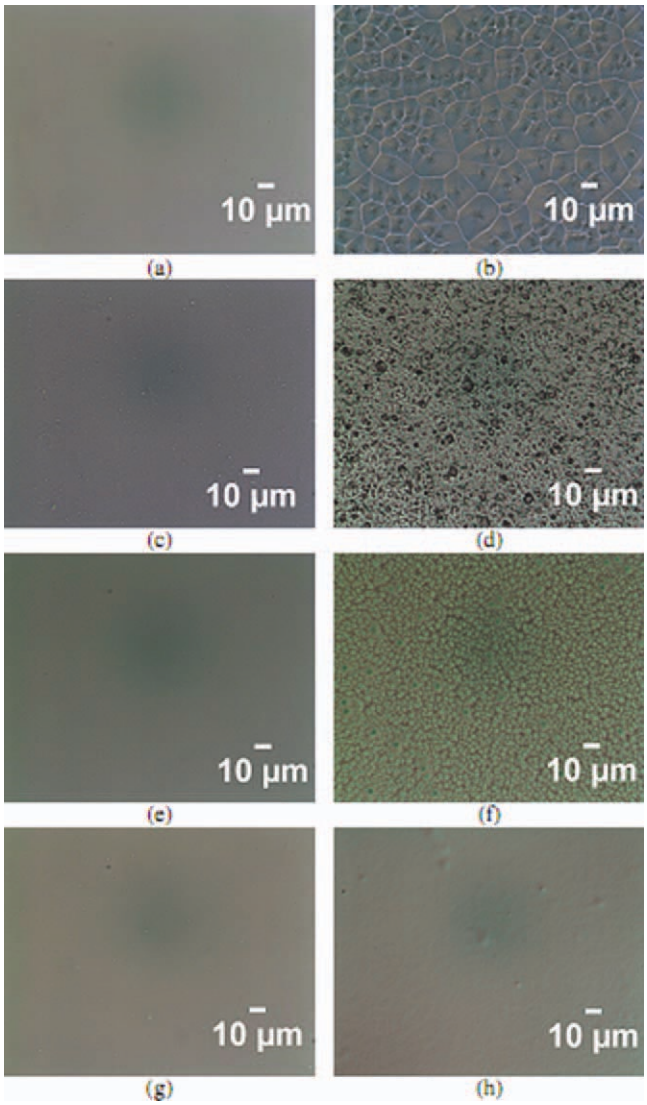

Figure 1 Optical microscope images (a) Flat LDPE homopolymer, (b) Rough LDPE homopolymer, (c) Flat EVA-12 copolymer, (d) Rough EVA-12 copolymer, (e) Flat EVA-28 copolymer, (f) Rough EVA-28 copolymer, (g) Flat EVA-40 copolymer, and (h) Rough EVA-40 copolymer at ×500 magnification. [Color figure can be viewed in the online issue, which is available at wileyonlinelibrary.com.]

XPS results

XPS measurements were made using two take-off angles of 0° and 60°. For a higher angle, the analyzed photoelectrons emerge from layers closer to the surface of the sample than for a lower angle. The thickness of the analyzed layer is ~ 5 nm at 60° take-off angle and about 10 nm at 0°. XPS analyses provide quantitative determination in depth of the composition of EVA surfaces as a function of VA content. Theoretical carbon and oxygen concentrations of EVA copolymers are given in Table II. Experimental results of the surface atomic carbon and oxygen concentrations for the flat and rough surfaces obtained from the XPS analysis at 0° and 60° take-off angles are also given in this table. (The presence of atomic oxygen in LDPE sample especially at 10 nm depth is attributed to any impurity present in this homopolymer which contains oxygen atom.). The surface oxygen concentration in EVA copolymers measured at take-off angle of 0° was 8–10% larger than the theoretical values for flat and 3–10% for rough EVA-12 and EVA-18 samples. However, the surface oxygen concentration in EVA copolymers measured at 0° take-off angle was 5–16% lower than the theoretical values for flat and 13–24% for rough EVA-28, EVA-33, and EVA-40 copolymer samples. These changes indicate that hydrophilic VA component enriched in EVA copolymer film surfaces below 18% VA content and hydrophobic PE component enriched at the surface for EVA-28, EVA-33, and EVA-40 samples for a depth of ~ 10 nm.

On the other hand, when XPS measurements are performed at 60° take-off angle, for a depth of ~ 5 nm, the atomic surface concentration of oxygen in all EVA copolymers at surface is lower than the theoretical values, 23–35% for flat EVA samples and 13–47% for rough EVA samples. These changes indicate that hydrophobic PE component enriched at the surface for all EVA samples for a depth of ~ 5 nm. In addition, the atomic oxygen concentrations obtained with take-off angle of 60° on all EVA samples were 23–30% lower than those obtained with take-off angle of 0° for flat samples and 16–30% for rough samples. These striking observations indicate that the hydrophobic PE was concentrated on the outermost surface layers at ~ 5 nm depth similar to the previously published results of Galuska.[42] It can be summarized that the order of atomic oxygen concentration was theoretical (bulk) > 10 nm > 5 nm

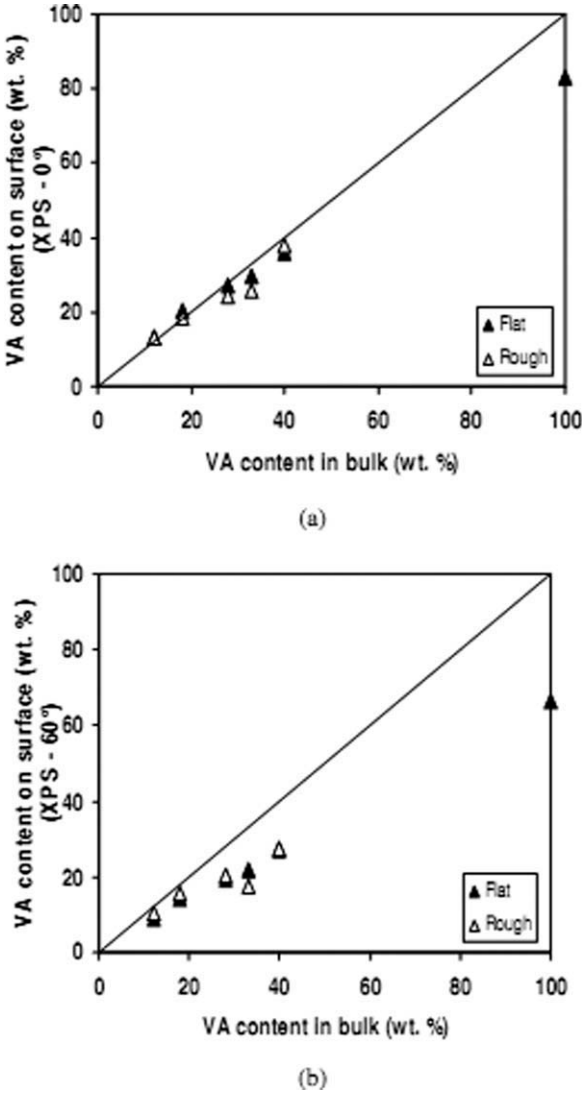

Figure 2 Change of VA content (wt %) on the surface with the change in VA content in the bulk copolymer for flat and rough coatings, when (a) 0° take-off angle of XPS and (b) 60° take-off angle of XPS was applied.

for EVA copolymers due to the enrichment of PE on the surface except EVA-12 and EVA-18 samples. The order of atomic oxygen concentration was 10 nm > theoretical > 5 nm for EVA-12 and EVA-18 samples indicating a sandwich-like structure where VA concentration was larger than the bulk concentration at ~ 10 nm layer but it decreased rapidly around 5 nm depth (less than the theoretical value) due to the enrichment of PE.

The surface VA contents (wt %) for flat and rough samples were calculated by using O/C ratios obtained from the XPS results at 0° and also 60° take-off angles. The variation of VA content on surface with the change in the VA content in the bulk copolymer for both flat and rough coatings at 0° and 60° take-off angles is given in Figure 2(a,b), respectively. It is clearly seen in Figure 2(b) that the XPS results obtained at 60° take-off angle (around 5 nm depth) were both less than the theoretical VA contents and also less than those obtained at 0° take-off angle (around 10 nm depth) given in Figure 2(a). This indicates that the surface segregation of the copolymer components was more pronounced at the outer layer having ~ 5 nm thickness; hence, the layer that was responsible for the measured contact angle and surface free energy properties of the copolymer surfaces.

On the other hand, the difference between the XPS results of the flat and rough surfaces was not significant for EVA samples except EVA-33 surface where the atomic oxygen content decreased 15% for 10 nm and 20% for 5 nm depth for rough surfaces. This is expected because angle resolved XPS is a good method to study the nanoscale surface composition and structure of the flat surfaces; however, it gives very complex results for rough surfaces. According to De Bernardez et al.,[49] the complexity of the XPS results on rough surfaces is due to two competitive mechanisms: (i) the shadowing effect of the neighboring clusters, which is the main effect and (ii) the electron emission from a tilted surface. Therefore, the XPS peak intensities are no straightforward for interpretation in case of rough substrates. It is possible that the exceptional behavior of the EVA-33 surface is due to its low molecular weight when compared with the other EVA samples. The melt flow index (MFI) is inversely proportional with the polymer molecular weight and EVA-33 has the largest MFI value than the other copolymers as seen in Table I, so it has the lowest molecular weight which allows more PE enrichment at the top surface layer. The molecular weight of EVA-40 copolymer is 42,000 g/mol as given in Ref. 50 and the MFI value of EVA-40 copolymer was approximately seven times smaller than that of the EVA-33 copolymer as seen in Table I showing that EVA-33 copolymer has a molecular weight which is lower than 42,000 g/mol.

Contact angle and surface free energy results

Advancing, θ_a, equilibrium, θ_e, and receding contact angle, θ_r results of water drops on flat and rough polymer coatings are given in Table III. Contact angle hysteresis, $\Delta\theta$ was calculated for each sample as the difference between θ_a and θ_r and also given in this table. $\Delta\theta$ indicates either the presence of chemical heterogeneity for flat surfaces or the surface roughness for chemically homogeneous surfaces.[1]

Flat LDPE homopolymer has a water drop equilibrium contact angle, $\theta_e = 102°$ and θ_e decreases with the increase of polar and hydrophilic VA content for flat EVA copolymer coatings and varies between 84° and 77° and finally $\theta_e = 60°$ for the flat PVAc

TABLE III
Contact Angle Results of Water Drops on Flat and Rough Polymer Surfaces and Solid Contact Area Fraction Values

		Flat samples				Rough samples			
Polymer	f_s^{CB}	θ_a	θ_e	θ_r	$\Delta\theta$	θ_a	θ_e	θ_r	$\Delta\theta$
LDPE	0.71	102	102	90	12	117	116	74	43
EVA-12	0.83	93	84	79	14	107	95	66	41
EVA-18	0.88	92	82	75	17	95	90	75	20
EVA-28	0.87	88	79	67	21	91	88	67	24
EVA-33	0.90	93	78	48	45	101	85	60	41
EVA-40	0.86	94	77	47	47	96	87	50	46
PVAc	N/A	80	60	34	46	N/A	N/A	N/A	N/A

homopolymer as seen in Table III. Our contact angle results are in concordance with the values reported in the literature. For example, $\theta_a = 93^\circ$ for flat EVA 12 sample which is very close to the results given in Refs. 45 and 47. θ_a was measured as 91° for rough EVA-28 and is similar to the value given in Ref. 43. It was determined that θ_e values on the rough samples of the same polymers are 7°–14° higher than the flat samples. This is due to the presence of partially trapped air pockets on the rough surfaces and also chemical heterogeneity arising from the VA content. $\Delta\theta$ values for the rough samples were much larger than that of the flat samples for LDPE and EVA-12 surfaces due to the partially trapped air pockets on these PE dominant rough surfaces.

Owens and Wendt[17] proposed a two-parameter equation by dividing the surface tension into dispersive, γ_{SV}^d and polar, γ_{SV}^p components based on the Fowkes[16] approach.

$$\gamma_{SV}^{tot} = \gamma_{SV}^d + \gamma_{SV}^p \quad (1)$$

$$\gamma_{LV}(1 + \cos\theta_e) = 2\left(\sqrt{\gamma_{SV}^d\ \gamma_{LV}^d} + \sqrt{\gamma_{SV}^p\ \gamma_{LV}^p}\right) \quad (2)$$

where γ_{LV} is the total surface tension of the liquid; γ_{LV}^d and γ_{LV}^p are dispersion and polar surface free energy components of the liquid, respectively. They proposed the use of only water and methylene iodide (CH_2I_2) drops to solve eq. (2). We reported θ_e results of test liquids on all of the flat samples in Table IV. Surface tension component values of test liquids are listed in Table V. We solved eq. (2) simultaneously for the two unknowns of γ_{SV}^p and γ_{SV}^d, then calculated the total surface tension of the polymer by using eq. (1). Surface free energy component results are given in Table VI in comparison with the literature result of Ref. 33. We plotted γ_{SV}^{tot} versus VA content (wt %) in bulk copolymer structure for flat polymer samples in Figure 3. As seen in this figure, γ_{SV}^{tot} increases from 32.3 up to 46.7 with the increase of VA content in bulk in agreement with the literature results.

Since Owens-Wendt equation cannot be used when nonasymmetric hydrogen-bonding interactions are present, van Oss-Good-Chaudhury[18,19] method was generally used for such cases. In this method, H-bonding interactions were considered as a subset of electron-acceptor and electron-donor interactions. The surface and interfacial free energies consisted of two components; a nonpolar or a Lifshitz-van der Waals component, γ_S^{LW} of electrodynamics origin and an acid–base component, γ_S^{AB} caused by acid–base (or H-bonding) interactions. γ_S^{tot} is then equal to the sum of these components,

$$\gamma_S^{tot} = \gamma_S^{LW} + \gamma_S^{AB} \quad (3)$$

γ_S^{AB} consists of electron-acceptor parameter, γ_S^+, and electron-donor parameter, γ_S^- and can be calculated as follows:

$$\gamma_S^{AB} = 2\sqrt{\gamma_S^+\ \gamma_S^-} \quad (4)$$

van Oss-Good-Chaudhury proposed a three-parameter equation to calculate the surface free energy of solids when three liquid drops are used and their γ_L^{LW}, γ_L^+, and γ_L^- values are known.

$$\gamma_L(1 + \cos\theta_e) = 2\left(\sqrt{\gamma_S^{LW}\ \gamma_L^{LW}} + \sqrt{\gamma_S^+\ \gamma_L^-} + \sqrt{\gamma_S^-\ \gamma_L^+}\right) \quad (5)$$

θ_e values of the test liquids other than water (methylene iodide, formamide, and ethylene glycol) on flat polymer samples are given in Table IV. Surface

TABLE IV
Equilibrium Contact Angle Results of Test Liquids on Flat Polymers

Polymer	θ_{Mel_2}	$\theta_{Formamide}$	θ_{EG}
LDPE	55	82	74
EVA-12	49	77	71
EVA-18	46	74	70
EVA-28	45	72	68
EVA-33	43	73	74
EVA-40	42	83	73
PVAc	41	43	54

TABLE V
Surface Tension Components of Test Liquids (mJ/m^2)

Liquid	γ_{LV}	γ_{LV}^d	γ_{LV}^p	γ_{LV}^{LW}	γ_{LV}^{AB}	γ_{LV}^+	γ_{LV}^-
Water	72.8	21.8	51.0	21.8	51.0	25.5	25.5
Ethylene glycol	48.0	–	–	29.0	19.0	1.92	47.0
Formamide	58.0	39.5	18.5	39.5	19.0	2.28	39.6
Methylene iodide	50.8	48.5	2.3	50.8	0	0	0

free energy components, γ_L^{LW}, γ_L^+, and γ_L^- of the four test liquids are given in Table V.[1,18] γ_S^{LW}, γ_S^+, and γ_S^- values of the polymer samples were calculated by using eq. (5) and the results are given in Table VII. For this purpose, we used four liquids (water, methylene iodide, formamide, and ethylene glycol) to form drops on sample surfaces while we were applying van Oss-Good-Chaudhury method. Initially, γ_S^{LW} was determined by using methylene iodide contact angle results which is a nonpolar liquid whose, γ_L^+, γ_L^- values are equal to 0 and then two other polar liquid pairs (water–formamide and water–ethylene glycol) were used to determine two sets of γ_s^+ and γ_s^- by using eq. (5). Later, we calculated the arithmetic averages of γ_s^+ and γ_s^- values from these sets. Since both Owens-Wendt[17] and van Oss-Good-Chaudhury[18,19] equations were derived to be applicable for only flat substrates, it is not convenient to apply these equations to considerably rough films having air pockets over the surface. Thus, no surface free energy calculation was done for the rough samples in our work.

The variation of oxygen atomic surface concentration for 60° take-off angle (around 5 nm depth), and electron donor parameter, γ_S^-, with the increase of VA content (wt %) in bulk for flat coatings is plotted in Figure 4. γ_S^- increases with the increase in VA content in bulk because of the hydrophilic and basic characteristics of the acetate group. The increase of the γ_S^- parameter with the increase of the carbonyl group present in a copolymer is also consistent with surface free energy analysis results of a block copolymer having amphoteric groups in its structure.[48]

TABLE VI
Surface Free Energy Results of Flat Polymer Surfaces Calculated by Using Owens-Wendt Equation (mJ/m^2)

	Calculated Results of this work			Literature results			
Polymer	γ_{SV}^p	γ_{SV}^d	γ_{SV}^{tot}	γ_{SV}^p	γ_{SV}^d	γ_{SV}^{tot}	Ref.
LDPE	0.1	32.2	32.3	2.0	28.6	30.6	33
EVA-12	3.8	31.6	35.4	4.1	31.9	36.0	33
EVA-18	4.2	32.9	37.1	N/A	N/A	N/A	N/A
EVA-28	5.4	32.8	38.2	5.1	32.6	37.7	33
EVA-33	5.6	33.7	39.3	N/A	N/A	N/A	N/A
EVA-40	5.9	34.0	39.9	5.4	33.0	38.4	33
PVAc	16.2	30.5	46.7	N/A	N/A	N/A	N/A

The polar interactions component, γ_{SV}^p calculated from the Owens-Wendt equation was also plotted with the VA content in bulk for the flat coatings in Figure 4. γ_{SV}^p increases with the increase of the VA content up to 16.2 mJ/m^2 when all our experimental results and the results given in Refs. 29, 33, and 39 were incorporated. It is realized that all the increase in γ_{SV}^{tot} for the flat copolymer surfaces was due to the increase in γ_{SV}^p since the variation of γ_{SV}^d was limited between 30.5 and 34.0 mJ/m^2 as seen in Table VI.

It is well known that when a polymer film is formed against a low-energy medium such as air, low-energy segments (PE for the EVA copolymer case) will migrate to the surface. If instead surface formation is done against a high-energy interface such as water, or a metal mold, then high-energy segments (VA for the EVA case) will migrate to the surface. EVA copolymers have dynamic surface properties above their glass transition temperatures, due to the high mobility of the VA segments. In our work, the surface enrichment of polyethylene segments occurred and is shown experimentally both in XPS and surface free energy results. XPS results obtained with the use of 60° take-off angle indicate that around 5 nm outer layer governs the contact angle and surface free energy of the prepared copolymers. The presence of the VA content on the surface has a direct effect on the contact angles and the corresponding γ_{SV}^p and γ_S^- values. As seen in Figure 4, the polar surface free energy component, γ_{SV}^p

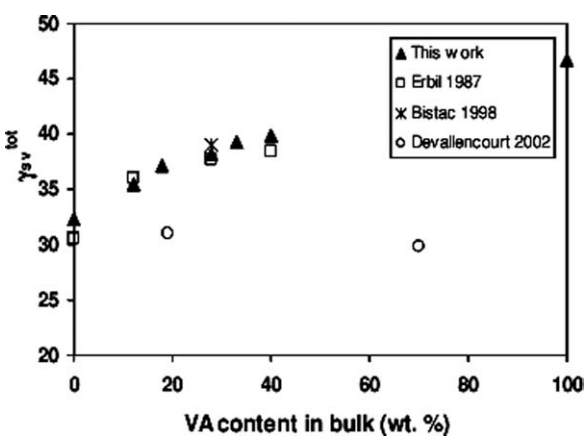

Figure 3 Change of the total surface free energy parameter, γ_{SV}^{tot} with the increase of VA content in bulk for experimental and literature data for the flat coatings.

TABLE VII
Surface Free Energy Results of Flat Polymer Surfaces Calculated by Using van Oss-Good Equation (mJ/m^2)

Polymer	γ_S^{LW}	γ_S^+	γ_S^-	γ_S^{AB}	γ^{tot}
LDPE	31.4	0.0	0.3	0.0	31.4
EVA-12	34.8	0.0	6.3	0.0	34.8
EVA-18	36.5	0.0	6.9	0.0	36.5
EVA-28	37.0	0.0	8.8	0.0	37.0
EVA-33	38.1	0.0	9.0	0.0	38.1
EVA-40	38.6	0.0	9.5	0.0	38.6
PVAc	39.1	0.2	22.1	4.2	43.3

gives better agreement with the XPS results obtained at the 60° take-off angle (around 5 nm depth) for the low VA contents, whereas electron donor parameter, γ_S^-, gives more coincidence with the XPS results for the high VA content samples.

We also tested both Wenzel[21] and Cassie-Baxter[22] equations which are generally used with the rough surfaces. The application of the Wenzel equation to our contact angle data on rough surfaces did not give reasonable results. According to Wenzel equation when the contact angle on a flat surface is less than 90°, then there should be a decrease in contact angle with the increase of the surface roughness, when air pockets are absent and complete wetting of the substrate takes place by the liquid drop.[21] However, we found the reverse in our experimental findings, indicating that the Wenzel equation cannot be applied for our contact angle results similar to recent findings by using micro-patterned surfaces.[51] Cassie and Baxter derived an equation for the equilibrium contact angle, θ_r^{CB} on a two-component composite smooth solid surface with varying degrees of heterogeneity in 1944.[22]

$$\cos\,\theta_r^{CB} = f_1\,\cos\,\theta_1 + f_2\,\cos\,\theta_2 = f_1\,\cos\,\theta_1 + (1-f_1)\,\cos\,\theta_2 \quad (6)$$

where f_1 and f_2 are the liquid/solid contact area fractions of solid components 1 and 2 on the surface, respectively. θ_1 and θ_2 are the equilibrium contact angles of the same liquid on each of the flat surfaces of these components. On the other hand, when air pockets are present on a rough single-component surface, Cassie-Baxter equation can also be used as follows:

$$\cos\theta_r^{CB} = (f_s^{CB})\ \left(1+\cos\theta_{flat}^{e}\right) - 1 \quad (7)$$

where f_s^{CB} is the fraction of the water/solid contact surface area and θ_{flat}^{e} is the equilibrium contact angle of water on flat surface of the same solid. f_s^{CB} is actually the ratio of the liquid/solid contact area under the droplet to the total projected area of the drop basement. According to eq. (7), the contact angle value on a rough surface θ_r^{CB} increases with the decrease of f_s^{CB}. Cassie-Baxter equation was found to be useful in the analysis of chemically heterogeneous flat surfaces, and also air pocket containing rough surfaces although it cannot explain the corrugation of the three-phase contact line between the drop and solid.[51] We calculated solid contact area fraction (f_s^{CB}) value by using the experimentally measured flat and rough water contact angles for the polymers having the same VA contents and the results are given in Table III. It is clearly seen from this table that (f_s^{CB}) increases from 0.7 to 0.9 with the increase of the VA content showing that the amount of partially trapped air pockets on the polymer surface rises with the increase of the PE content when rough surfaces are obtained from EVA copolymers by the dip coating method.

CONCLUSIONS

Sixty degrees take-off angle XPS results which corresponds to 5 nm depth show the surface enrichment of the hydrophobic PE component on all flat and rough EVA surfaces and the near-surface region is dominated by a PE rich layer, whereas hydrophilic VA component was enriched on the surface when VA $<$ 18% for only at 10 nm depth. On the other hand, the difference between the XPS results of the flat and rough surfaces was not significant for EVA samples except EVA-33 surface. It is possible that the exceptional behavior of the EVA-33 surface where the atomic oxygen content decreased 15% for 10 nm and 20% for 5 nm depth for rough surfaces was due to its low molecular weight when compared with the other EVA samples.

On the rough samples, the contact angle hysteresis values were much larger than that of the flat samples for LDPE and EVA-12 surfaces due to the

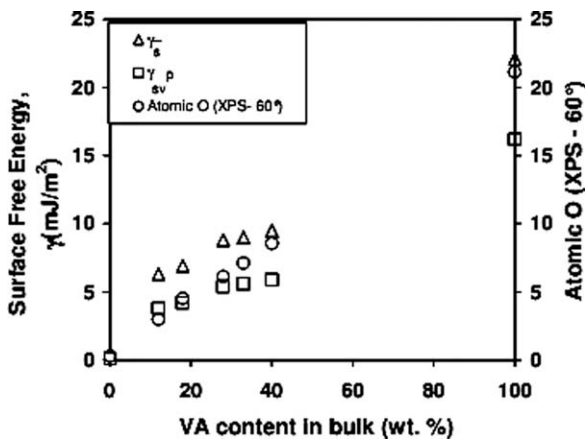

Figure 4 Change of the oxygen atomic surface concentration for 60° take-off angle, electron donor parameter, γ_S^-, and polar interactions component, γ_{SV}^p, with the increase of the VA content in bulk for the flat coatings.

presence of partial trapping of air pockets on these rough surfaces. γ_{SV}^{p} and γ_S^- values increased with the increase of the VA content for the flat EVA copolymer coatings due to the presence of polar and basic acetate groups. When XPS results are compared with the surface free energy component results calculated from the van Oss-Good-Chaudhury method, a good agreement was found between the basic surface free energy component, γ_S^-, and atomic surface concentration of oxygen at the 5 nm top surface layers of the EVA copolymers especially for samples having high VA contents.

References

1. Erbil, H. Y. Surface Chemistry of Solid and Liquid Interfaces; Blackwell Publishing: Oxford, 2006.
2. Adamson, A. W.; Gast, A. P. Physical Chemistry of Surfaces; Wiley: New York, 1997.
3. Blades, C. E.; Skeist, I. Handbook of Adhesives; Van Nostrand Reinhold Company: New York, 1977.
4. Brushan, B.; Jung, Y. C. Prog Mater Sci 2011, 56, 1.
5. Erbil, H. Y.; Demirel, A. L.; Avci, Y.; Mert, O. Science 2003, 299, 1377.
6. Lu, X.; Zhang, C.; Han, Y. Macromol Rapid Commun 2004, 25, 1606.
7. Lu, X.; Zhang, J.; Zhang, C.; Han, Y. Macromol Rapid Commun 2005, 26, 637.
8. Lu, X.; Tan, S.; Zhao, N.; Yang, S.; Xu, J. J Colloid Interface Sci 2007, 311, 186.
9. Kang, X.; Zi, W. W.; Xu, Z. G.; Zhang, H. L. Appl Surf Sci 2007, 253, 8830.
10. Yao, Y.; Dong, X.; Hong, S.; Ge, H.; Han, C. C. Macromol Rapid Commun 2006, 27, 1627.
11. Puukilainen, E.; Koponen, H. K.; Xiao, Z.; Suvanto, S.; Pakkanen, T. A. Colloids Surf A Physicochem Eng Asp 2006, 287, 175.
12. Puukilainen, E.; Rasilainen, T.; Suvanto, M.; Pakkanen, T. A. Langmuir 2007, 23, 7263.
13. Rasilainen, T.; Suvanto, M.; Pakkanen, T. A. Surf Sci 2009, 603, 2240.
14. Ucar, I. O.; Cansoy, C. E.; Erbil, H. Y.; Pettitt, M. E.; Callow, M. E.; Callow, J A. Biointerphases 2010, 5, 75.
15. Girifalco, L. A.; Good, R. J. J Phys Chem 1957, 61, 904.
16. Fowkes, F. M. Ind Eng Chem 1964, 56, 40.
17. Owens, D. K.; Wendt, R. C. J Appl Polym Sci 1969, 13, 1741.
18. Van Oss, C. J.; Chaudhury, M. K.; Good, R. J Chem Rev 1988, 88, 927.
19. Van Oss, C. J.; Good, R. J. Langmuir 1992, 8, 2877.
20. Erbil, H. Y. Polymer 1996, 37, 5483.
21. Wenzel, R. N. Ind Eng Chem 1936, 28, 988.
22. Cassie, A. B. D.; Baxter, S. Trans Faraday Soc 1944, 40, 546.
23. Salyer, I. O.; Kenyon, A. S. J Polym Sci Part A-1: Polym Chem 1971, 9, 3083.
24. Erbil, H. Y. Vinyl Acetate Emulsion Polymerization and Copolymerization with Acrylic Monomers; CRC Press: USA, 2000.
25. Henderson, A. M. IEEE Electr Insul Mag 1993, 9, 30.
26. Gao, L. Y.; Wu, S. Z.; Tu, D. M.; Kao, K. C. Proceedings of the 21th Symposium on Electrical Insulating Materials, Japan, 1988; p 59.
27. McEvoy, R. L.; Krause, S. J Appl Polym Sci 1997, 64, 2221.
28. Arsac, A.; Carrot, C.; Guillet, J. J Therm Anal Cal 2000, 61, 681.
29. Devallencourt, C.; Marais, S.; Saiter, J. M.; Labbe, M.; Métayer, M. Polym Test 2002, 21, 253.
30. Wang, L.; Fang, P.; Ye, C.; Feng, J. J Polym Sci Part B: Polym Phys 2006, 44, 2864.
31. Bai, Y.; Qian, J.; An, Q.; Zhu, Z.; Zhang, P. J Membr Sci 2007, 305, 152.
32. Matsunaga, T.; Tamai, Y. J Appl Polym Sci 1978, 22, 3525.
33. Erbil, H. Y. J Appl Polym Sci 1987, 33, 1397.
34. Dann, J. R. J Colloid Interface Sci 1970, 32, 302.
35. Park, S. J.; Kim, H. C.; Kim, H. Y. J Colloid Interface Sci 2002, 255, 145.
36. Roe, R. J. J Phys Chem 1965, 69, 2809.
37. Roe, R. J. J Phys Chem 1968, 72, 2013.
38. Grundke, K.; Jacobasch, H. J.; Simon, F.; Schneider, S. T. J Adhes Sci Technol 1995, 9, 327.
39. Bistac, S.; Kunemann, P.; Schultz, J. J Colloid Interface Sci 1998, 201, 247.
40. Briggs, D.; Beamson, G. Anal Chem 1993, 65, 1517.
41. Chihani, T.; Bergmark, P.; Flodin, P. J Adhes Sci Technol 1993, 7, 327.
42. Galuska, A. A. Surf Interface Anal 1994, 21, 703.
43. Chihani, T.; Bergmark, P.; Flodin, P. J Adhes Sci Technol 1995, 9, 843.
44. McEvoy, R. L.; Krause, S.; Wu, P. Polymer 1998, 39, 5223.
45. Cepeda-Jimenez, C. M.; Torregrosa-Macia, R.; Martin-Martinez, J. M. J Adhes Sci Technol 2003, 17, 1145.
46. Martinez-Garcia, A.; Sanchez-Reche, A.; Gisbert-Soler, S.; Cepeda-Jimenez, C. M.; Torregrosa-Macia, R.; Martin-Martinez, J. M. J Adhes Sci Technol 2003, 17, 47.
47. Landete-Ruiz, M. D.; Martin-Martinez, J. M. Int J Adhes Adhesives 2005, 25, 139.
48. Erbil, H. Y.; Yasar, B.; Suzer, S.; Baysal, B. M. Langmuir 1997, 13, 5484.
49. De Bernardez, L. S.; Ferron, J.; Goldberg, E. C.; Buitrago, R. H. Surf Sci 1984, 139, 541.
50. Lee, W. L.; Hong, M.; Widjaja, E.; Loo, S. C. J. Macromol Rapid Commun 2010, 31, 1193.
51. Erbil, H. Y.; Cansoy, C. E. Langmuir 2009, 25, 14135.